



PERGAMON

Pattern Recognition 34 (2001) 1417–1428

PATTERN
RECOGNITION

THE JOURNAL OF THE PATTERN RECOGNITION SOCIETY

www.elsevier.com/locate/patcog

Robust detection of skewed symmetries by combining local and semi-local affine invariants

Dinggang Shen^a, Horace H.S. Ip^{b,*}, Eam Khwang Teoh^c

^aDepartment of Radiology, Johns Hopkins University, MD 21287, USA

^bImage Computing Group, Department of Computer Science, Tat Chee Ave, City University of Hong Kong, Kowloon, Hong Kong

^cSchool of Electrical and Electronic Engineering, Nanyang Technological University, Singapore 639798, Singapore

Received 22 December 1999; received in revised form 28 March 2000; accepted 28 March 2000

Abstract

Affine-invariant feature vector (Ip and Shen Image Vision Comput. 16 (2) (1998) 135–146), that captures both local and semi-local geometric features around each point of the object boundary is applied here for the detection of skewed symmetries. Based on the affine-invariant shape representation, the problem of detecting symmetry axes has been formulated as a problem of detecting lines, with known orientations, in a local similarity matrix of an object. Since the feature vector extracts sufficient local and semi-local shape information for every point along the object boundary, the process of checking symmetric point pairs is thus robust against both noises and deformations. Moreover, our technique is able to detect *all* the local reflectional symmetries contained in the object. Various experimental results have shown the robustness and effectiveness of our method in detecting skewed symmetries from both *self-symmetric* objects and *generalized* objects. © 2001 Pattern Recognition Society. Published by Elsevier Science Ltd. All rights reserved.

Keywords: Skewed symmetry; Local invariants; Semi-local invariants; Rotational symmetry; Reflectional symmetry

1. Introduction

Symmetry identification is a useful means for analyzing and recognizing objects, since many objects in both the man-made world and nature exhibit some degrees of symmetry [1]. Skewed symmetry is the type of pattern that usually emerges when viewing a symmetric planar shape obliquely. Usually, the term is restricted to orthographic viewing directions, and the distribution induced by projection can be modeled by a 2D affine transformation. The problem of detecting skewed symmetries has received a lot of attentions in machine vision literature, since symmetric feature was understood early

on that the presence of such cue helps in performing a wide variety of tasks such as grouping, deprojection, and object recognition [2,3]. Also, based on the symmetry of an object, human beings can infer its structure and estimate its pose (orientation and positions) in the 3D space, even when certain parts of the object are lost or occluded.

Rotational symmetry and reflectional symmetry are two commonly studied forms of symmetries. In [4], we have established the relationship between reflectional symmetry and rotational symmetry, that is, the number of reflection-symmetric axes is either *zero* or *K* for any rotationally symmetric image with *K* folds, where $K \geq 1$.

The detection of skewed symmetries has been investigated by many researchers in the past [5,6]. Based on the nature of the features extracted from a shape, the existing methods for symmetry detection can be roughly classified into two general approaches [5], namely, global versus local approach. Global approach considers the entire

* Corresponding author. Tel.: + 852-2788-8641; fax: + 852-2784-4916.

E-mail addresses: dgshen@cbmv.jhu.edu (D. Shen), cship@cityu.edu.hk (H.H.S. Ip), eekteoh@ntu.edu.sg (E.K. Teoh).

contour when finding the axes of skewed symmetries, examples of this approach can be found in [2,5]. Local approach uses locally defined distinctive features, such as local invariants computed at a single point on the curves [1,7], or methods that statistically compare pairs of contour points [8,9]. The advantage and disadvantage associated with local versus global approach is well reported in the computer vision literature: local approach can work even when certain parts of the curves are occluded or missing, while the global approach in general severely suffers from occlusion. Global approach is insensitive to noise, while local approach is unstable and sensitive to noise unless a multi-scale approach is adopted [10]. Representation of object contour by B-spline is one of the methods for restraining noises [11]. In addition, the amount of local information is insufficient for robust matching. To overcome some of the disadvantages relating to both global and local approaches, Sato and Cipolla [12] proposed integral invariants based on group invariant parameterisation. They show that integral invariants do not suffer from occlusion problem and are less sensitive to noise than differential invariant.

In our previous work [4], we developed a close-form solution, based on the generalized complex (GC) moments [13], to detect the global symmetric axes for both reflectional and rotational symmetries. The major results of this work are that we developed (a) theorems that allow us to determine whether an input shape is symmetric or not; (b) algorithms that detect the axes of symmetries; and (c) a constraint relationship that link the numbers of reflectional and rotational symmetries. Since GC moments provide a global description of a shape, this approach is unsuitable for detecting the axes of local symmetry (or skewed symmetry) and is also sensitive to occlusion or missing parts.

Separately, our work on affine invariant active contour [14] yields a new area-based shape representation scheme which is affine invariant as well as able to capture both local and global shape characteristics. Based on this new shape representation, we formulated an affine invariant active contour model (which we call AI-snake) for affine invariant model-based segmentation [14]. The approach has also been applied to the retrieval of shapes [15]. Given the ability of the affine invariant shape representation developed in [14] to capture both local and semi-local shape characteristics, it opens up the possibility of applying it to skewed and local symmetry detection.

In this paper, we develop techniques for the detection of both local and global symmetries and skewed symmetries, using the affine invariant representation developed in [14]. Based on this representation, the detection of skewed symmetries is simplified as a procedure of detecting lines, with known orientations, within a local similarity matrix of an object. Compared to the symmetry detection technique that is based only on local invariant

[1], our method is robust against noise and deformation, because of the combined utilization of both local and semi-local affine invariants.

The paper is organized as follow. The formulation of an area-based shape representation and the definition of a feature vector that is able to capture both local and semi-local shape features are briefly reviewed in Section 2. Based on this definition, section 3 describes our approaches for detecting skewed rotational and reflectional symmetries. The proposed approach can detect the actual fold number and all the axes of rotational symmetries for the rotationally symmetric shapes, even severely corrupted. Also in section 3, a similar approach for the detection of *all* (global or local) axes of reflectional symmetries is presented. A rich number of experiments on detecting skewed symmetries are given in Section 4. This paper concludes in Section 5.

2. An affine invariant area-based feature vector

In the followings, we will review our development of an affine invariant feature that will form the basis for our detection of skewed symmetries.

The contour of image object C can be represented by a parametric equation $r(t) = [x(t), y(t)]^T$, where t is the parameter and $r(t)$ is a column vector. Both t_1 and t_2 used in the following are also the parameter of the contour. $\dot{r}(t)$ and $\ddot{r}(t)$ are the first and second derivatives of the contour. Their definitions are

$$\dot{r}(t) = [\dot{x}(t) \quad \dot{y}(t)]^T = \begin{bmatrix} \frac{dx(t)}{dt} & \frac{dy(t)}{dt} \end{bmatrix}^T,$$

$$\ddot{r}(t) = [\ddot{x}(t) \quad \ddot{y}(t)]^T = \begin{bmatrix} \frac{d^2x(t)}{dt^2} & \frac{d^2y(t)}{dt^2} \end{bmatrix}^T.$$

Under general affine transformations, the following three expressions are relatively invariant,

$$|(r(t) - r(t_1)) \quad (r(t) - r(t_2))|, \quad |(r(t) - r(t_1)) \quad \dot{r}(t)|,$$

$$|\dot{r}(t) \quad \ddot{r}(t)|$$

where $|\cdot|$ denotes determinant of matrix. That is, their values remain unchanged up to a factor that only depends on the parameters of the affine transformation applied. This factor is actually the determinant of the affine transformation. In this paper, we will use

$$\frac{1}{2} |\dot{r}(t) \quad \ddot{r}(t)| = \frac{1}{2} (\dot{x}(t)\ddot{y}(t) - \ddot{x}(t)\dot{y}(t))$$

to establish a relatively-affine-invariant feature vector for every point along the object boundary.

The first and second derivatives of $x(t)$ and $y(t)$ with respect to t can be approximately written as

$$\dot{x}(t) = \frac{dx(t)}{dt} \doteq \frac{x(t) - x(t - \Delta t)}{\Delta t}$$

$$\ddot{x}(t) = \frac{d^2x(t)}{dt^2} \doteq \frac{x(t) - 2 \cdot x(t - \Delta t) + x(t - 2 \cdot \Delta t)}{\Delta t \cdot \Delta t}$$

$$\dot{y}(t) = \frac{dy(t)}{dt} \doteq \frac{y(t) - y(t - \Delta t)}{\Delta t}$$

$$\ddot{y}(t) = \frac{d^2y(t)}{dt^2} \doteq \frac{y(t) - 2 \cdot y(t - \Delta t) + y(t - 2 \cdot \Delta t)}{\Delta t \cdot \Delta t}$$

Using the above approximations, we can obtain

$$\frac{1}{2} |\dot{r}(t) \quad \ddot{r}(t)| \doteq \frac{1}{2} \begin{vmatrix} x(t - 2 \cdot \Delta t) & x(t - \Delta t) & x(t) \\ y(t - 2 \cdot \Delta t) & y(t - \Delta t) & y(t) \\ 1 & 1 & 1 \end{vmatrix}$$

The above expression indicates that the value of $\frac{1}{2} |\dot{r}(t) \quad \ddot{r}(t)|$ denotes the area of a triangle, formed by three vertices $(x(t - 2 \cdot \Delta t), y(t - 2 \cdot \Delta t))$, $(x(t - \Delta t), y(t - \Delta t))$ and $(x(t), y(t))$.

In fact, the area of any triangle is relatively affine invariant and the ratios of such areas are affine invariant:

$$area_{t_1, t_2, t_3} = \frac{1}{2} \begin{vmatrix} x(t_1) & x(t_2) & x(t_3) \\ y(t_1) & y(t_2) & y(t_3) \\ 1 & 1 & 1 \end{vmatrix}$$

where $area_{t_1, t_2, t_3}$ is the area of a triangle, whose three vertices are $(x(t_1), y(t_1))$, $(x(t_2), y(t_2))$ and $(x(t_3), y(t_3))$.

Accordingly, an affine-invariant feature vector can be designed for every feature point of the given contour. Let $\{(x_1, y_1), (x_2, y_2), \dots, (x_N, y_N)\}$ be the set of feature points representing the given shape C in a particular scale. These feature points can be extracted from the sample points, which are evenly distributed along the *affine-length* shape boundary [1]. To make the feature points robust against noises, we take the same number of points from both sides of a sample point and average them to obtain a feature point. For the i -th feature point (x_i, y_i) , its corresponding feature vector is defined as

$$F_i = [f_{1i} \quad f_{2i} \quad \dots \quad f_{Mi}]^T,$$

where $f_{ji} = \frac{1}{2} \begin{vmatrix} x_{[i-j]} & x_i & x_{[i+j]} \\ y_{[i-j]} & y_i & y_{[i+j]} \\ 1 & 1 & 1 \end{vmatrix}$ is the area of a triangle

formed by $(x_{[i-j]}, y_{[i-j]})$, (x_i, y_i) , and $(x_{[i+j]}, y_{[i+j]})$, and $[i+j] = (i+j)\%N$, $[i-j] = (i-j+N)\%N$. The size of M in effect determines the sampling resolution of the curve for our representation. As to f_{ji} , if j is close to l ,

f_{ji} denotes local feature, i.e. f_{ji} (for small j) extracts information of local shape centered on the point (x_i, y_i) , which is sensitive to noise. As j increases, f_{ji} gradually captures the semi-local features of the curve, i.e. f_{ji} extracts low frequency (smooth) information of the shape, which is less sensitive to digitization noise. Therefore, F_i captures both local and semi-local information around the i -th feature point of the curve.

Furthermore, F_i can be made affine invariant by the following normalization:

$$\hat{F}_i = \frac{F_i}{\sum_{i=1}^N \sum_{j=1}^M |f_{ji}|},$$

where $\hat{F}_i = [\hat{f}_{1i} \quad \hat{f}_{2i} \quad \dots \quad \hat{f}_{Mi}]^T$.

Thus, the contour of an object, C , can be described by a set of affine-invariant feature vectors,

$$\{\hat{F}_i, i = 1, 2, \dots, N\}.$$

In the following, we will propose techniques for detecting skewed symmetric axes based upon them.

3. Detection of skewed symmetries: problem formulation

3.1. Properties of the feature vectors under rotational symmetry and reflectional symmetry

The above section has already given the definition of an affine invariant feature vector for every feature point on the contours. In the following, we will show that, in theory a pair of rotational symmetric points (or a pair of reflection-symmetric points) own the same feature vectors. Furthermore, we show that both the detection of rotational symmetries and the detection of reflectional symmetries can be done by detecting the continuous lines of 1s with slope +1 (for rotational symmetries) and slope -1 (for reflectional symmetries) within a local similarity matrix. This greatly simplifies the process of detecting symmetric axes.

For discussion purpose, in Fig 1, we use symbol V_i to represent the i -th feature point (x_i, y_i) and let two points V_i and V_k be a pair of reflection-symmetric points, and two points V_i and V_l be a pair of rotationally-symmetric points. From the definition of \hat{f}_{ji} given in section 2, it is easy to show $\hat{f}_{ji} = \hat{f}_{jk} = \hat{f}_{jl}$. Using the normalized feature element, \hat{f}_{ji} , which is invariant to affine transformation, the equality $\hat{f}_{ji} = \hat{f}_{jk} = \hat{f}_{jl}$ holds even under affine transformations.

Thus, once the set of feature vectors for a contour has been extracted, the detection of skewed symmetries becomes the process of comparing the similarity on each pair of feature vectors. In what follows, the properties respectively on reflection-symmetric and rotationally-symmetric pairs are formalized.

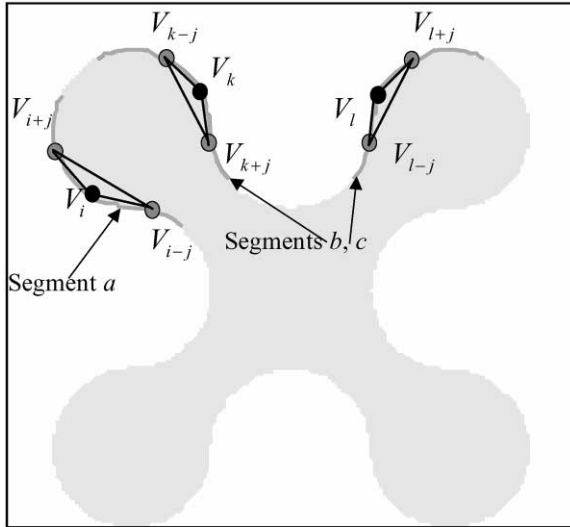


Fig. 1. Properties of affine invariant features on rotational and reflectional symmetries. Points V_i and V_k are the pair of reflection-symmetric points, while points V_i and V_l are the pair of rotationally-symmetric points.

3.2. Property of rotational symmetry

For *rotationally symmetric object*, if the l -th feature point corresponds to the i -th feature point, the feature vector \hat{F}_l of the l -th point is expected to be identical to the feature vector \hat{F}_i of the i -th point. That is, the matching error $E_{i,l}$ between the i -th and l -th feature points should be zero, i.e.,

$$E_{i,l} = (\hat{F}_l - \hat{F}_i)^T \cdot G \cdot (\hat{F}_l - \hat{F}_i) = 0,$$

where $1 \leq i, l \leq N$ and G is an $M \times M$ diagonal matrix defined by a Gaussian function, i.e.

$$G = [g_{mm}]_{M \times M} \quad \text{and} \quad g_{mm} = \frac{1}{\sqrt{2\pi\sigma}} e^{-((m/M - 1/2)^2 / 2\sigma^2)}$$

In fact, G is a weighting matrix used for controlling the contributions from different feature elements.

For simplification, we use a *local similarity measure* $S_{i,l}$ to represent the similarity of feature point pair. A definition of $S_{i,l}$ can be obtained from the matching error $E_{i,l}$ as follow,

$$S_{i,l} = 1 - \frac{E_{i,l}}{\text{Max}_{1 \leq i,l \leq N} E_{i,l}} \quad (1)$$

From the above definition, it is easy to observe that the value of $S_{i,l}$ is also invariant to any affine transformation.

The above definition implies $S_{i,l} = 1$ if the l -th feature point is the corresponding rotationally-symmetric point

of the i -th feature point. Furthermore, in Fig. 1, we assume that segment a passing through the i -th feature point V_i is rotationally symmetric to the segment c passing through the l -th feature point V_l . In this case, the $[i+h]$ -th and $[l+h]$ -th feature points respectively on the segments a and c are also the corresponding rotationally-symmetric points. This means, $S_{[i+h],[l+h]}$ should also be 1 (i.e. $S_{[i+h],[l+h]} = 1$), where h is an integer and $[i+h] = (i+h+N) \% N$. Consequently, if we visualize the local similarity matrix, $S = [S_{i,l}]$, as an image with intensities between 0 and 1 (level 1 means *white*), then, in the ideal case, we would observe in this image a *continuous* white line (i.e. line of 1s) passing through the position (i, l) with slope equal to $+1$ (see Figs. 2(d1) and (d2) for example).

In practice, since noise and deformation on the input shape may occur, the similarity between the feature vectors of the corresponding rotationally-symmetric points, $S_{i,l}$, may not be exactly 1. To cater for noise, as well as variability in the sample point selection and to make allowance for deformation, we instead look for high intensity lines with slope $+1$ in the image produced by the local similarity matrix.

3.3. The property of reflectional symmetry

Similarly, if the k -th feature point V_k is the reflection-symmetric point of the i -th feature point V_i , then the matching error, $E_{i,k}$, between the corresponding feature vectors will be zero, i.e.

$$E_{i,k} = (\hat{F}_k - \hat{F}_i)^T \cdot G \cdot (\hat{F}_k - \hat{F}_i) = 0.$$

With the same normalization in (1), the similarity measure $S_{i,k} = 1$ can be obtained for two reflection-symmetric points based on the above definition of the matching error. In Fig. 1, if the segment a passing through the feature point V_i is reflection-symmetric to the segment b passing through the feature point V_k , then $S_{[i+h],[k-h]}$ should be 1. Here, h is an integer, and the $[i+h]$ -th and $[k-h]$ -th feature points are localized respectively on the segments a and b . Similarly, we can observe a *continuous* white line (line of 1s) passing through the position (i, k) with slope -1 in the image of local similarity matrix.

The detection of reflectional symmetries can thus be implemented efficiently by searching for a line of 1s with slope -1 in the matrix of similarity measures. See Fig. 2(e1, e2) for example.

The above observations mean that once the local similarity matrix has been computed for a curve, the detection of rotational symmetry (or the detection of reflectional symmetry) of the curve can be achieved by simply searching for *continuous* straight line segments with slope $+1$ (or -1) within the local similarity matrix.

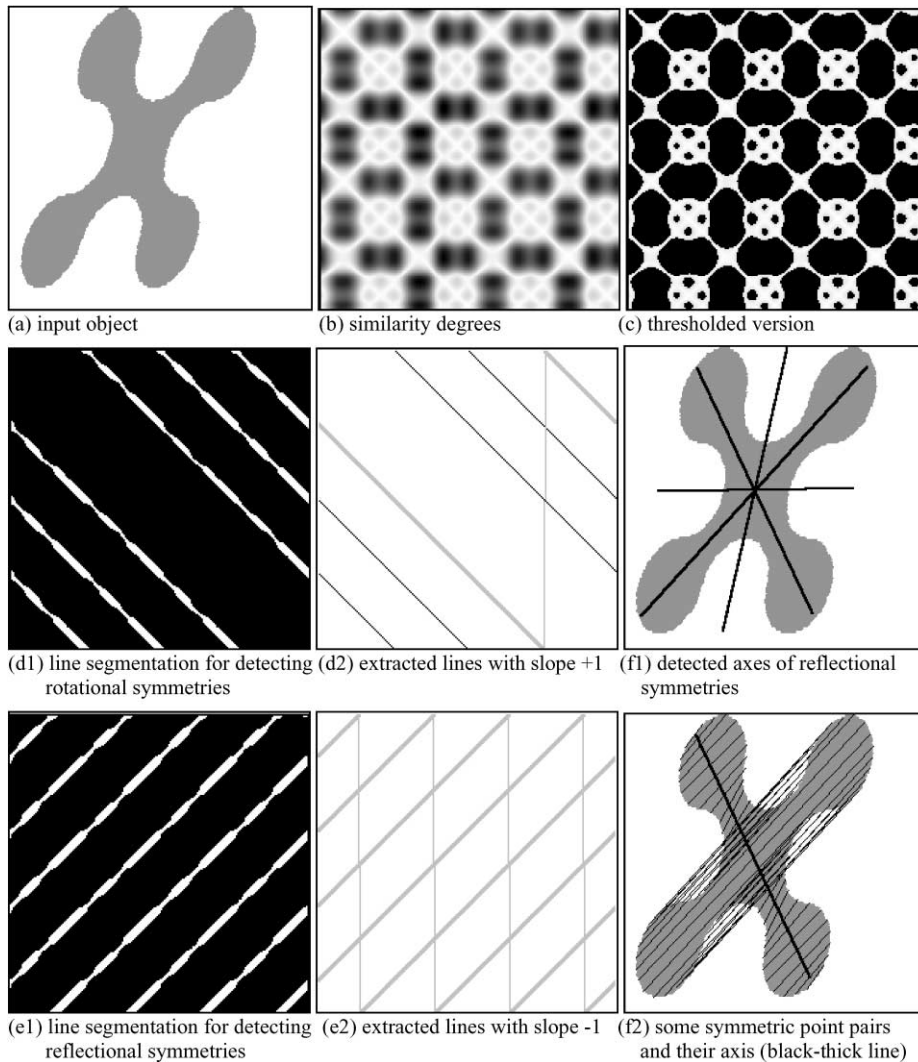


Fig. 2. Skewed symmetry detection for an object, where fold number and skewed axes of reflectional symmetries are detected. Thick-black lines in (e2) represent the *selected* correct symmetric axes. The vertical thin lines in (d2) and (e2) are used for connecting the logically-same lines.

3.4. Process of detecting rotational symmetries

With noises and deformation, the feature vectors of symmetric points are typically not exactly the same. This leads to a local similarity matrix such as the one shown in Fig. 2(b), for an object shown in Fig. 2(a), with values falling between 0 and 1.

Since theory tells us that the lines of 1s with slope +1 in the local similarity matrix indicates the locations of local (skewed) symmetry axes (Fig. 2(b)), the first step is to binarise the local symmetry matrix at a suitable threshold value. In our experiments, we set our threshold at $S_{i,l} = 0.85$. Using this threshold, we can get a binarised local similarity matrix, where $S_{i,l} = 0$ if

$S_{i,l} < 0.85$. Fig. 2(c) is the thresholded similarity image from Fig. 2(b).

Given the thresholded local similarity matrix, it is easy to detect all line segments with slope +1 and -1 within it through suitable spatial filtering such as morphological opening and closing with a line structuring element. Among these extracted straight line segments is one corresponding to $S_{i,i} = 1$ which corresponds to comparing a feature vector of a feature point with itself. This line is the diagonal line of the binarised local similarity matrix, which we call the *identity line*. Removing this line, we get a segmented image, such as the one shown in Fig. 2(d1). Fig. 2(d2) is the result of fitting lines to the segmented image.

An important observation is that if the length of the detected line is equal to N (the total point number on the contour), then the input object must be rotationally symmetric and its fold number is equal to “the number of complete lines *plus 1*”. For example, the number of the complete lines in Fig. 2(d2) is 3, then the fold number of the object is 4.

Finally, we can summarize an *algorithm* for the rotational symmetry detection, based on the concept of the local similarity matrix:

- (1) Binarised the local similarity matrix.
- (2) Detect lines within it with slope $+1$ using line fitting procedure.
- (3) Remove the *identity* line.

- (4) Calculate the number of the fitted lines with length N . The fold number is exactly “the number of complete lines *plus 1*”.

3.5. Process of detecting reflectional symmetries

The algorithm for detecting a pair of reflection-symmetric points and their axes are similar to the above algorithm for detecting rotational symmetries. And, *both the process of detecting rotational symmetries and the process of detecting reflectional symmetries are operating on the same similarity matrix*. The main differences are as follows. *One* difference is that, in rotational symmetry detection, we look for the lines with slope $+1$ in the

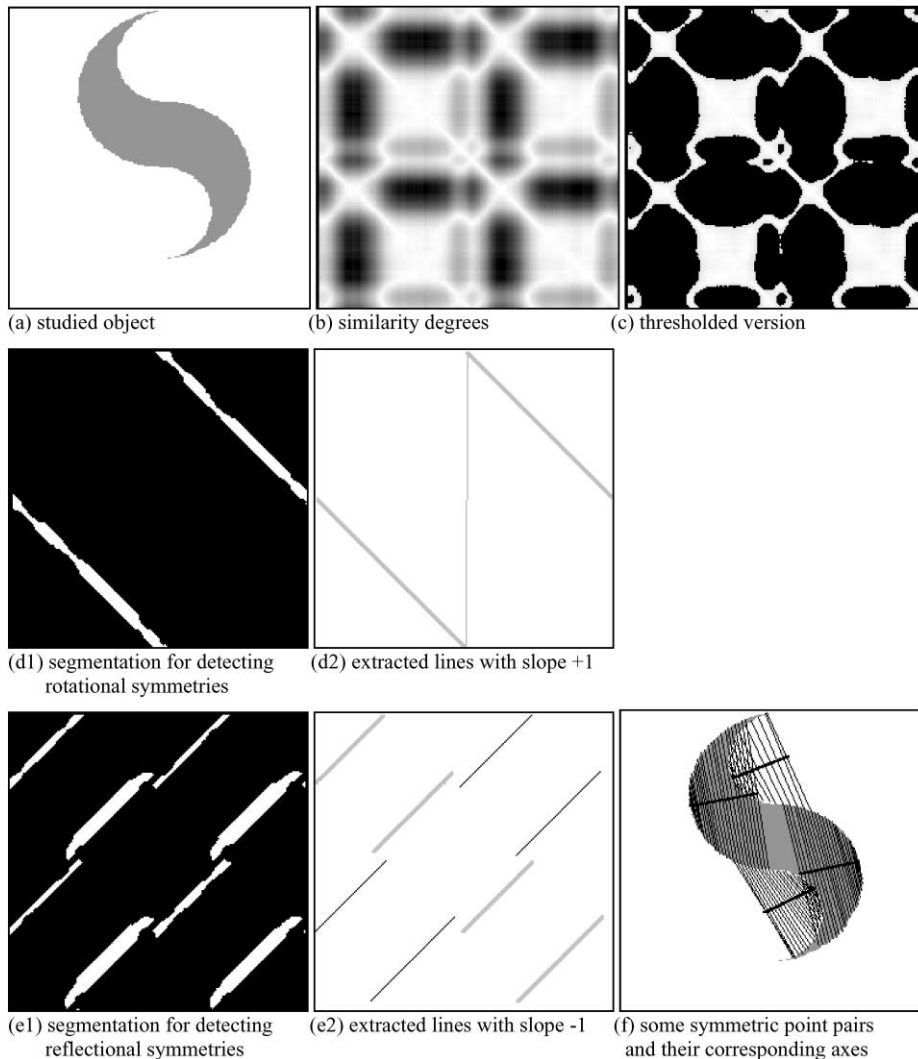


Fig. 3. Symmetry detection for the object which is rotationally symmetric but globally not reflection-symmetric. The vertical thin line in (d2) is used for connecting the logically-same line. Grey thick lines in (e2) represent the *selected* correct symmetric axes. In (e2), four black thin lines are not selected, since they don't satisfy the constraint condition of being reflection-symmetric.

similarity image, while in reflectional symmetry detection we look for the lines with slope -1 . Another difference is that, in reflectional symmetry detection, we should establish a constraint condition for confirming the actual local reflectional symmetry. Since there may exist many local reflectional symmetries in an object, such as Fig. 3(a), we should choose only the significant local symmetries from a set of potential candidates. A possible constraint condition for this is that the pairs of reflection-symmetric points should be on the *same continuous* segment, which is commonly studied by researchers. For example, in Fig. 3(e2), only four grey thick lines satisfy this constraint condition. Other four thin lines do not meet this requirement. In addition, the axis for the pairs

of reflection-symmetric points can be determined by the middle points of all pairs, using Least Mean Square Error.

An *algorithm* for detecting reflectional symmetry based on the local similarity matrix can be summarized below:

- (1) Binarised the local similarity matrix.
- (2) Detect significant line segments within it with slope -1 using line fitting procedure.
- (3) Select fitted lines satisfying the constraint condition that the pairs of reflection-symmetric points should be on the *identical continuous* segment, and with at least a certain length.
- (4) Calculate the axis of every reflectional symmetry.

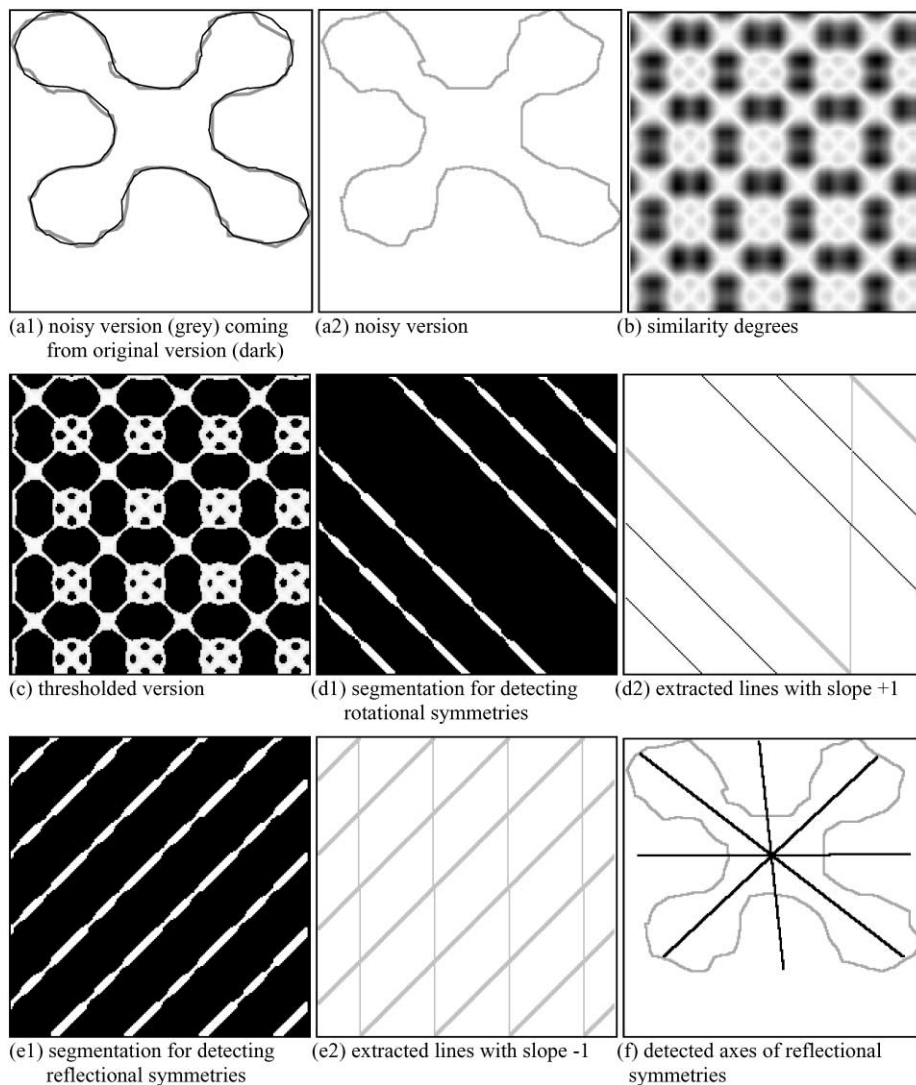


Fig. 4. Symmetry detection for the noisy object, corrupted from object in Fig. 2(a).

4. Experimental results

In this section, we will provide a series of experimental results on skewed and local symmetry detection. The

proposed algorithm is tested by (a) an object that is both rotationally symmetric and reflection-symmetric (Fig. 2), (b) an object that is only rotationally symmetric but locally reflection-symmetric (Fig. 3), and their corrupted

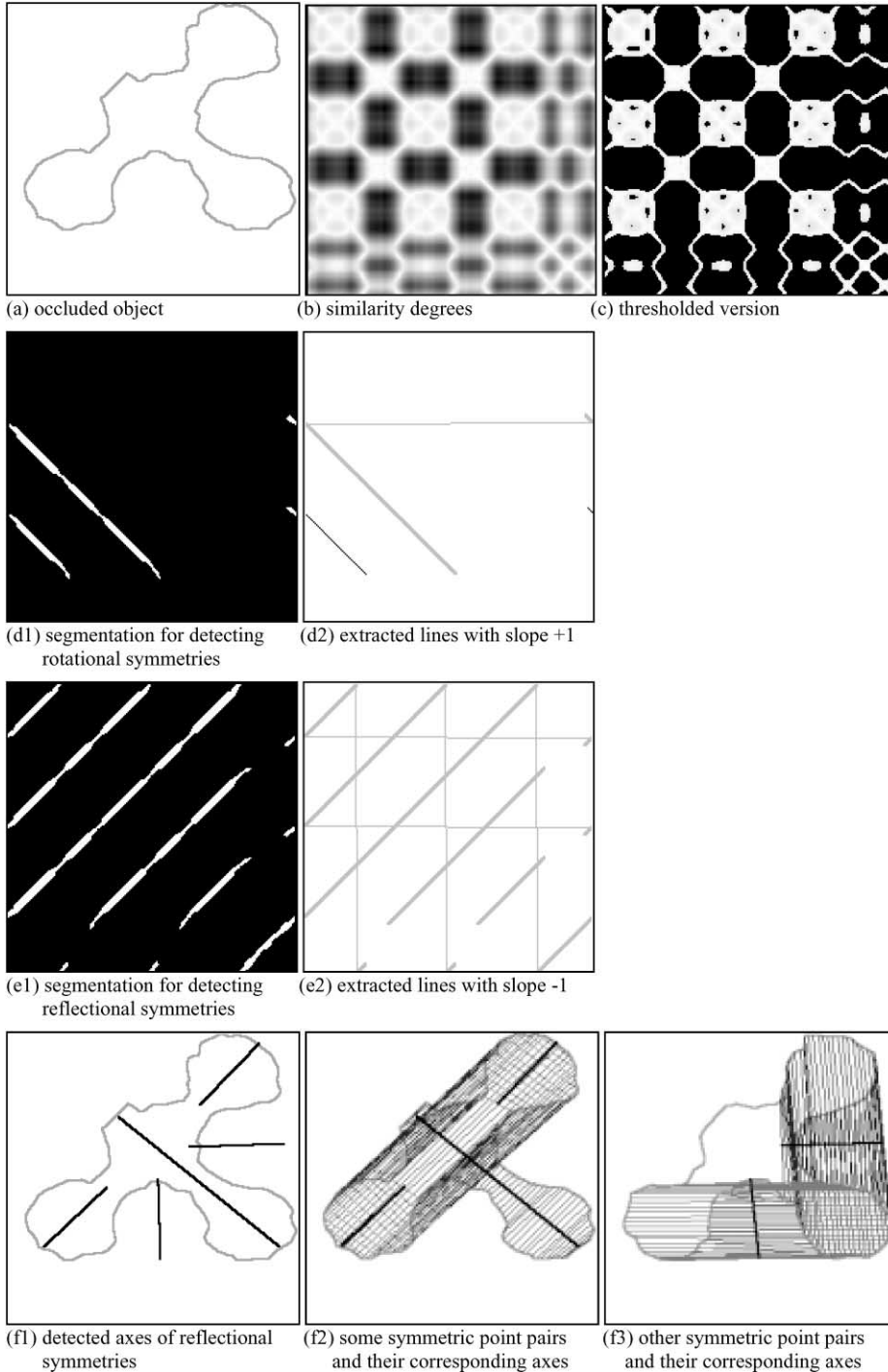


Fig. 5. Detection of skewed symmetries for the occluded object, cut from object in Fig. 2(a).

and occluded versions (Figs. 4, 5 and 6). Also, our technique is tested on some general object shapes, such as the fish shown in Fig. 7. The numbers of feature points, N , on the object boundaries vary from 200 to 400 for different objects. And, the size of M is set to 30 for all cases in our experiments.

4.1. Detection of rotational symmetries:

All the objects used in Figs. 2–4 and 6 are skewed rotationally symmetric, our method can correctly detect the fold numbers for all these objects. Although the object in Fig. 4(a1, a2) is corrupted by noise, the rotational symmetry, including the fold number, still can be detected correctly. It is easy to see from Fig. 4(a2) that the

contour of the object was severely corrupted by noise. Since the proposed method uses the combined information of local and semi-local features around every feature point of the object, the result of skewed symmetries detection is very robust against noise and deformations. Also, in Fig. 6, the contour of the object was also severely corrupted by noise. The local similarity matrix in Fig. 6(c) appears to be quite complicated, but the line detection result (Fig. 6(d1)) is still satisfactory since we are only interested in lines with slope equal to $+1$ and -1 . On the other hand, the two objects shown in Figs. 5 and 7 are not rotationally symmetric, since no significant line segment (line with length equal N) with slope $+1$ exists in the binarised local similarity matrices (Fig. 5(d1, d2), 7(d1, d2)).

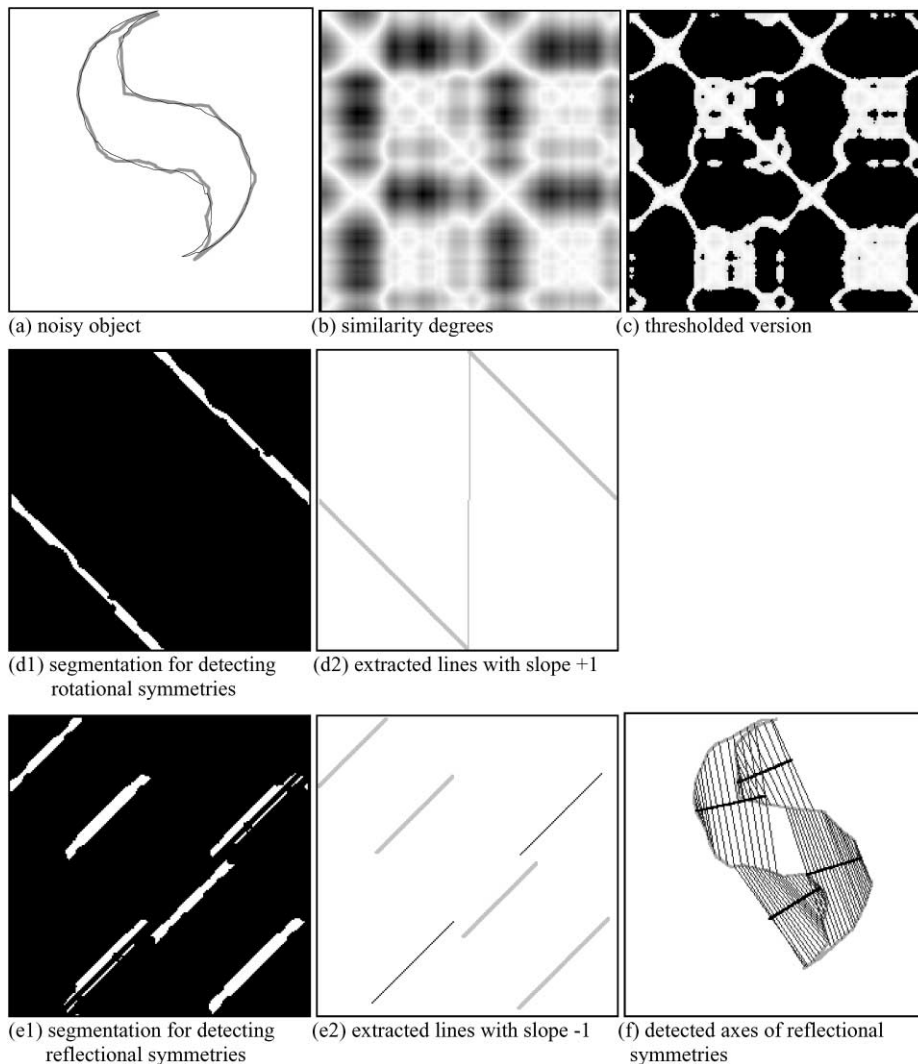


Fig. 6. Symmetry detection for a noisy object, corrupted from object in Fig. 3(a).

4.2. Detection of both global and local skewed reflectional symmetries

Objects in Figs. 2 and 4 are globally reflection-symmetric. Object in Fig. 4(a1, a2) is the noisy version of the object in Fig. 2(a). Our technique successfully detected the axes of skewed reflectional symmetry for both figures. The detected axes for these two objects are respectively shown in Fig. 2(f1) and Fig. 4(f).

Figs. 3(a) and 6(a) show the same object. The difference is being that the contour of object in Fig. 6(a) is corrupted by noise. Even under noise, the detected local reflectional symmetries in Fig. 6(f) are the same to those in

Fig. 3(f). Notice some of the candidate lines in Figs. 3(e2) and 6(e2) were eliminated by the constraint condition for reflectional symmetry.

Object in Fig. 5(a) shows an occluded and corrupted version of Fig. 2(a). The global and local reflectional symmetries are correctly detected for the corrupted figure. In Fig. 5(e2), vertical and horizontal thin lines are used to connect the logically-identical lines. Fig. 5(f1) shows the axes of the detected reflectional symmetries. The symmetric point pairs for different local symmetries are respectively shown in Fig. 5(f2, f3).

Fig. 7(a) gives a general object shape, i.e. a fish. Its local similarity matrix is quite complicated whereas the result

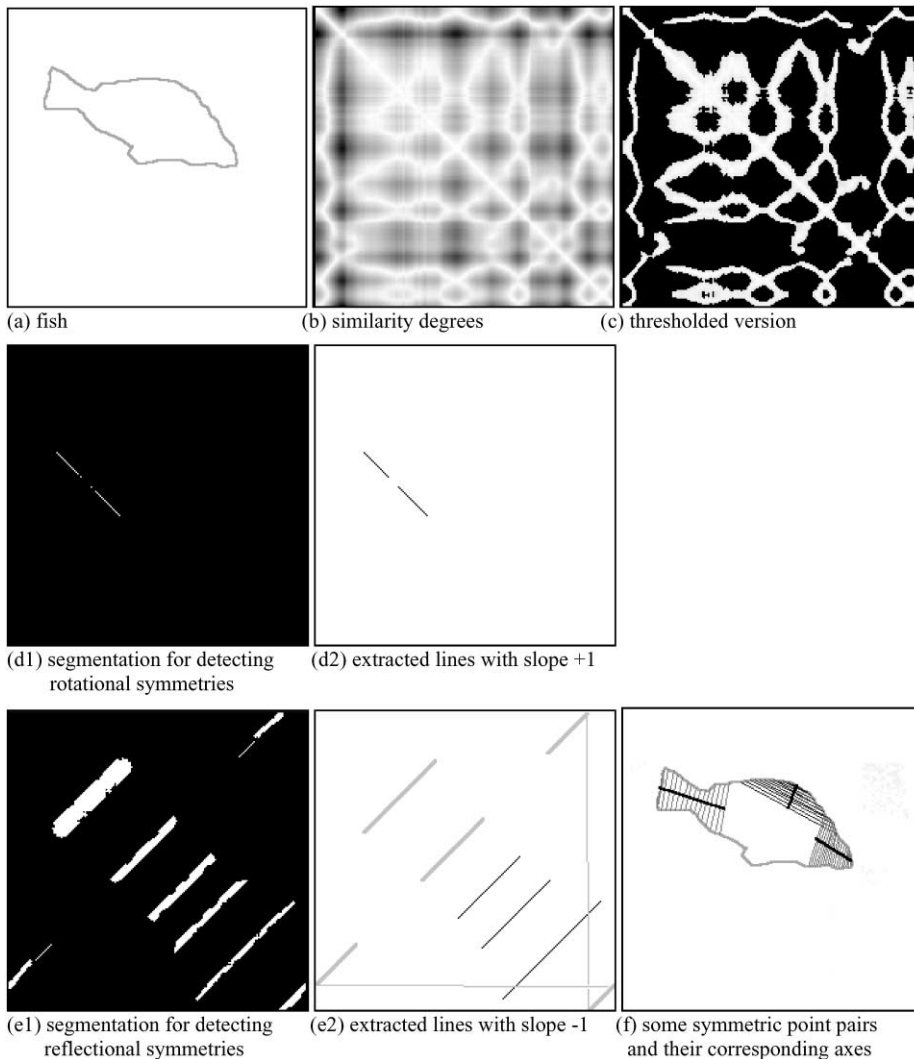


Fig. 7. Symmetry detection for the generalized object, where no global rotational symmetry and reflectional symmetry exist. The vertical and horizontal thin lines in (e2) are used for connecting the same line. Grey thick lines in (e2) represent the *selected* correct symmetric axes. In (e2), three black thin lines are not selected, since they don't satisfy the constraint condition of being reflection-symmetric.

of the detected line segments is still satisfactory. Our technique gives three local reflectional symmetries for this object in Figs. 7(f).

5. Conclusion

In this paper, we present an approach for detecting both rotational symmetries and reflectional symmetries based on a single local similarity matrix. A local similarity measure is developed from a set of affine-invariant feature vectors that capture both local and semi-local geometric information around the points of the object boundary. Since the feature vectors are affine invariant, our approach is also affine invariant and thus applicable in detecting both local and global skewed symmetries. Moreover, since the feature vector captures not only local invariants but also semi-local invariants of the object, this makes our approach robust against noise, deformation, and occlusion. Various experiments, on typical self-symmetric objects and general objects, have demonstrated the robustness and effectiveness of our technique in detecting skewed symmetries.

Acknowledgements

This work is supported by a HKSAR Competitive Earmarked Research Grant No: 9040437.

References

- [1] L. van Gool, T. Moons, D. Ungureanu, E. Pauwels, Symmetry from shape and shape from symmetry, *Int. J. Robotics Res.* 14 (5) (1995) 407–424.
- [2] S.A. Friedberg, Finding axes of skewed symmetry, *Comput. Vision Graphics Image Process.* 34 (1986) 138–155.

- [3] T. Kanade, Recovery of the 3D-shape of an object from a single view, *Artif. Intell.* 17 (1981) 409–460.
- [4] Dinggang Shen, H.S. Horace Ip, K.T. Kent Cheung, Eam Khwang Teoh, Symmetry detection by generalised complex (GC) moments: a close-form solution, *IEEE Trans. Pattern Anal. Mach. Intell.* 21 (5) (1999) 466–476.
- [5] A.D. Gross, T.E. Boult, Analyzing skewed symmetries, *Int. J. Comput. Vision* 13 (1994) 91–111.
- [6] A.M. Bruckstein, D. Shaked, Skew-symmetry detection via invariant signatures, *Pattern Recognition* 31 (2) (1998) 181–192.
- [7] L. van Gool, T. Moons, D. Ungureanu, A. Oosterlinck, The characterisation and detection of skewed symmetry, *Comput. Vision Image Understanding* 61 (1) (1995) 138–150.
- [8] T.J. Cham, R. Cipolla, Symmetry detection through local skewed symmetries, *Image Vision Comput.* 13 (5) (1995) 439–450.
- [9] K.S.Y. Yuen, W.W. Chan, Two methods for detecting symmetries, *Pattern Recognition Lett.* 15 (3) (1994) 279–286.
- [10] F. Mokhtarian, Silhouette-based object recognition with occlusion through curvature scale space, *Proceedings of the European Conference on Computer Vision*, Cambridge, UK, Vol. I, 1996, pp. 566–578.
- [11] P. Saintmarc, H. Rom, G. Medioni, B-spline contour representation and symmetry detection, *IEEE Trans. Pattern Anal. Mach. Intell.* 15 (11) (1993) 1191–1197.
- [12] J. Sato, R. Cipolla, Affine integral invariants for extracting symmetry axes, *Image Vision Comput.* 15 (8) (1997) 627–635.
- [13] H.H.S. Ip, Dinggang Shen, Generalized affine invariant image normalization, *IEEE Trans. Pattern Anal. Mach. Intell.* 19 (5) (1997) 431–440.
- [14] H.H.S. Ip, Dinggang Shen, An affine-invariant active contour model (AI-snake) for model-based segmentation, *Image Vision Comput.* 16 (2) (1998) 135–146.
- [15] Dinggang Shen, W.H. Wong, H.H.S. Ip, Affine invariant image retrieval by correspondence matching of shapes, *Image Vision Comput.* 17 (7) (1999) 489–499.

About the Author—DINGGANG SHEN received his BS, MS and Ph.D. degrees in Electronics Engineering from Shanghai JiaoTong University (SJTU) in 1990, 1992 and 1995, respectively. He worked as Research Assistant in the Department of Computer Science at the Hong Kong University of Science & Technology from December 1994 to June 1995. From Sep. 1995 to Feb. 1996, he was a Lecturer of Communication Engineering at Shanghai JiaoTong University. He was a Research Fellow in the Department of Computer Science at City University of Hong Kong, from Feb. 1996 to Aug. 1997. From June 1997 to Feb 1999, he worked first at Post-Doctoral Fellow and then as Research Fellow in School of Electrical and Electronic Engineering at Nanyang Technological University, Singapore. Since Jan 1999, he worked as Postdoctoral Research Fellow in School of Medicine at Johns Hopkins University, doing medical imaging. His research interests are in the areas of computer vision, pattern recognition, image processing, neural network and image indexing & retrieval. Dr. Shen has published over 60 articles in journals and proceedings of international conferences.

About the Author—PROF. HORACE H.S. IP received his B.Sc. (First Class Honours) degree in Applied Physics and Ph.D. degree in Image Processing from University College London, United Kingdom, in 1980 and 1983 respectively. Presently, he is the Professor and Head of the Computer Science Department and the director for Centre for Innovative Applications of Internet and Multimedia Technologies (AIMtech Centre) of City University of Hong Kong. His research interests include image processing and analysis, pattern recognition, hypermedia computing systems and computer graphics. Dr. Ip is a member of the Editorial Board of the *Pattern Recognition Journal* (Elsevier), the *International Journal of Multimedia Tools and Applications* (Kluwer Academic), and the *Chinese Journal of CAD and Computer Graphics* (The Chinese Academy of Science) and a guest editor of the international journal of *Real-Time Imaging* (Academic Press). Prof. Ip serves on the IAPR Governing Board and co-chairs its Technical Committee on Multimedia

Systems. He was the Chairman of the IEEE (HK) Computer chapter, and the Founding President of the Hong Kong Society for Multimedia and Image Computing. He has published over 100 papers in international journals and conference proceedings.

About the Author—EAM KHWANG TEOH received his B.E. and M.E. degrees in Electrical Engineering from the University of Auckland, New Zealand in 1980 and 1982 respectively and the Ph.D. degree in Electrical & Computer Engineering from the University of Newcastle, New South Wales in 1986. Presently, he is a Vice-Dean and an Associate Professor in the School of Electrical and Electronic Engineering, Nanyang Technological University, Singapore. He is a co-inventor of an Australian Patent on An Adaptive Thickness Controller for a Rolling Mill. His current research interests are in the field of Computer Vision and Pattern Recognition, Intelligent Systems, Robotics and Industrial Automation. He has published more than 150 journal and conference papers in these areas.